

1 **SUPPLEMENTARY INFORMATION**

2

3 **Expression of CD20 after Viral Reactivation Renders HIV-Reservoir Cells**
4 **Susceptible to Rituximab**

5

6 Carla Serra-Peinado, Judith Grau-Expósito, Laura Luque-Ballesteros, Antonio Astorga-Gamaza,
7 Jordi Navarro, Jenny Gallego-Rodriguez, Mario Martin, Adrià Curran, Joaquin Burgos, Esteban
8 Ribera, Berta Raventós, Rein Willekens, Ariadna Torrella, Bibiana Planas, Rosa Badía, Felipe
9 Garcia, Josep Castellví, Meritxell Genescà, Vicenç Falcó, and Maria J. Buzon

10

11

12

13

14

15

16

17

18

19

20

21 **Table S1.** Clinical data of patients included in the study.

Patient ID (new)	Time since HIV diagnosis (months)	CD4 Cell Count (cells/ μ l)	%CD4	Viral Load (copies/ml)	Time on ART (months)	ART regimen
1	300	580	20.19	<50	122	DRV/c
2	50	1,120	40.2	<50	28	TDF+FTC+DRV/r
3	11	280	22.45	<50	4	ABC+3TC+DTG
4	25	1,030	34.87	<50	16	TDF+FTC+EVG/c
5	146	1,830	51.37	<50	48	EFV+TDF+3TC
6	267	1,020	55.21	<50	120	FTC+NVP+TDF
7	166	1,180	40.85	<50	88	FTC+RPV+TDF
8	245	1,060	-	<50	179	FTC+RPV+TDF
9	66	990	45.96	<50	21	TDF+FTC+RPV
10	36	1,150	47.33	<50	19	TDF+FTC+RPV
11	240	150	-	<50	156	c/DRV
12	247	1,050	32.03	<50	206	c/DRV
13	216	1,150	38.31	<50	170	c/DRV
14	298	1,200	-	<50	176	COB/DRV
15	10	680	39.7	<50	10	ABC+3TC+RPV
16	32	280	22	<50	27	TDF+FTC+RPV
17	43	790	35.4	<50	21	TDF+FTC+EVG/c
18	48	800	40.42	<50	23	ABC+3TC+RAL
19	46	2,290	27.8	<50	25	ABC+3TC+RPV
20	31	1,230	55.8	<50	26	ABC+3TC+RPV
21	279	330	15.98	<50	18	TDF+FTC+EVG/c
22	30	130	7.38	<50	25	ABC+3TC+RAL
23	30	1,290	61.79	<50	23	TDF+FTC+RPV
24	40	530	27	<50	21	TDF+FTC+RPV
25	56	990	42.56	<50	33	TDF+FTC+DRV/r
26	47	490	36.57	<50	18	ABC+3TC+RPV
27	78	1,210	45.93	<50	29	TDF+FTC+EVG/c
28	153	770	49.03	<50	51	EFV+FTC+TDF
29	292	560	-	<50	156	COB+DRV+RTG
30	340	1,040	-	<50	168	DRV+FTC+RTV+TDF
31	94	600	10.3	<50	40	DRV+RTV
32	115	360	30	<50	61	LPV+RTV
33	72	800	-	<50	18	3TC+ABV+DTG
34	33	490	-	<50	28	EVG+FTC+TAF/c
35	31	560	-	<50	11	EVG+FTC+TAF/c
36	49	1,070	-	<50	40	EFV+FTC+TDF
37	31	810	-	<50	22	3TC+ABV+DTG
38	42	1,150	-	<50	37	3TC+ABV+RPV
39	13	1,760	-	<50	13	EVG+FTC+TAF/c
40	55	970	-	<50	45	3TC+ABC+DTG
41	28	910	33.97	<50	22	TDF+FTC+EVG/c
42	17	750	35.79	<50	16	ABC+3TC+RPV
43	24	-	-	<50	23	TDF+FTC+EFV

44	25	600	31.23	<50	17	ABC+3TC+ATV/r
45	132	740	-	<50	79	3TC+ABC+DTG
46	136	710	-	<50	115	3TC+ABC+DTG
47	106	810	-	<50	101	3TC+ABC+RPV
48	310	340	-	<50	79	DRV+FTC+TDF/c
49	59	800	-	<50	41	FTC+RPV+TDF
50	66	1,130	-	<50	19	EVG+FTC+TAF/c
51	42	430	-	<50	38	EVG+FTC+TAF/c
52	300	2,020	-	<50	-	3TC+ABV+DTG
53	129	270	-	<50	126	3TC+DTG
54	319	689	-	<50	136	DRV+ETV+RTG/r
55	111	600	-	<50	105	FTC+RPV+TDF
56	1042	1,010	24.7	<50	624	3TC+ABV+DTG
57	750	180	18.75	<50	112	3TC+ABC+DTG
58	306	1,080	39.5	<50	273	3TC+ABV+RPV
59	67	715	39.72	<50	66	FTC+RPV+TDF
60	8	420	30.46	74,500	-	UNT
61	72	320	22.09	47,300	-	UNT
62	0	570	26.41	60,300	-	UNT
63	2	600	24.69	296,000	-	UNT
64	84	330	8.89	79,200	-	UNT
65	0	610	36.88	119,000	-	UNT
66	0	480	18.27	178,000	-	UNT
67	0	960	37.03	145,000	-	UNT
68	0	920	41.2	9,560	-	UNT
69	226	240	9.65	272	-	UNT
70	0	430	23.2	3,850,000	-	UNT
71	0	480	26.27	12,800,000	-	UNT
72	3	190	38.82	23,300,000	-	UNT
73	67	790	35.43	20,300	-	UNT
74	44	760	21.09	11,000	-	UNT
75	36	760	30.17	22,700	-	UNT
76	218	360	19.79	880	-	UNT
77	197	170	6.93	517,000	-	UNT
78	205	280	18.25	250,000	-	UNT
79	2	180	4.36	405,000	-	UNT
80	0	780	27.1	302,000	-	UNT
81	1	550	42.71	92	-	UNT
82	0,1	150	7.5	5,000,000	-	UNT
83	85	314	17	56,000	-	UNT
84	88	368	20.5	56,000	-	UNT
85	51	407	21.04	14,000	-	UNT
86	0	310	-	80,400	-	UNT

22 FTC, emtricitabine; TDF, tenofovir; NVP, nevirapine; ATV, atazanavir; 3TC, lamivudine; EFV, efavirenz; ABC, abacavir; RAL, raltegravir;

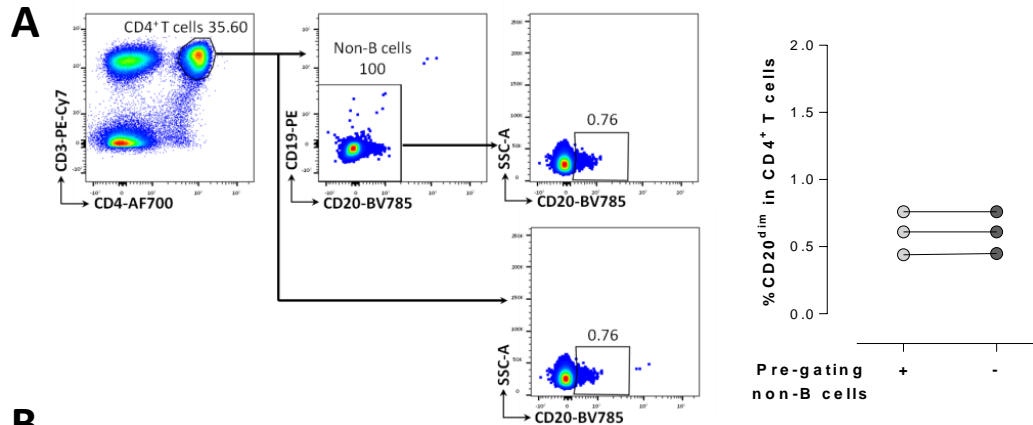
23 EVG, elvitegravir; DTG, dolutegravir; DRV, darunavir; RPV, Rilpivirine; TAF, tenofovir alafenamida; LPV, Lopinavir; /r, boosted with

24 ritonavir; /c, boosted with cobicistat; UNT, untreated.

25

Supplementary Figure 1

26

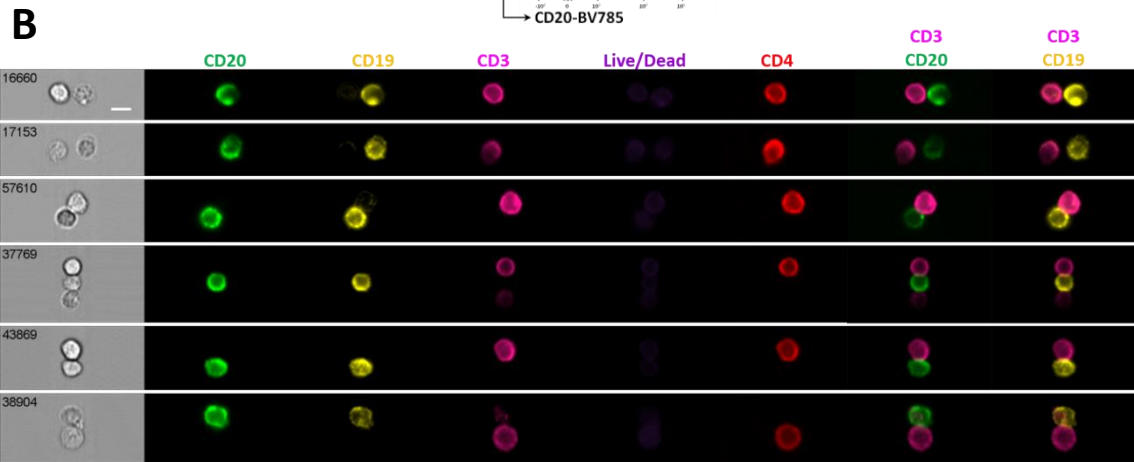


27

28

29

30



31

32

33

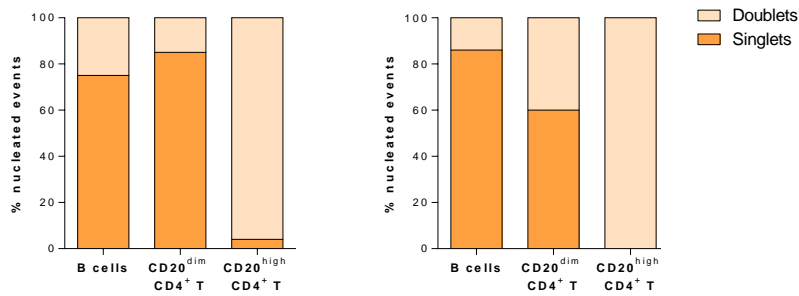
34

35

36

Patient #9

Patient #22

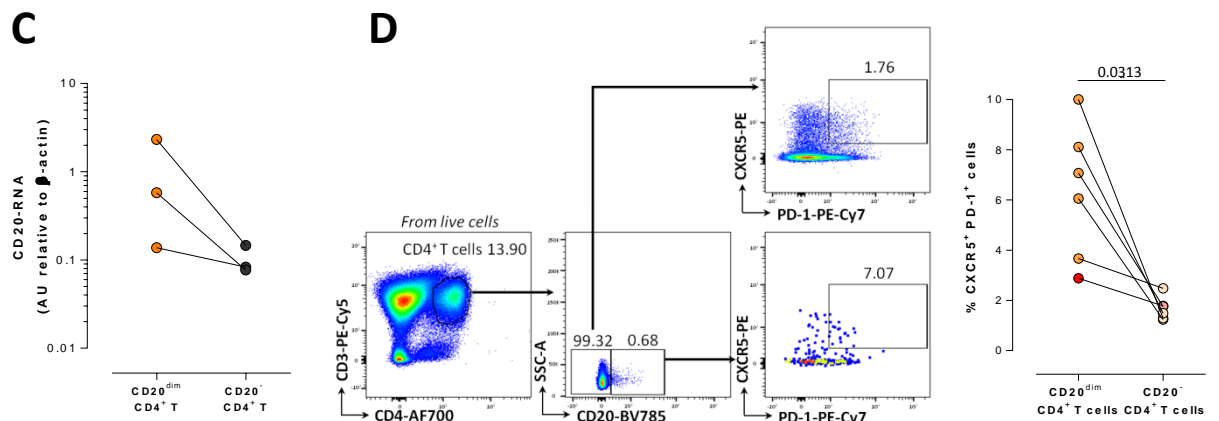


37

38

39

40



41

42

43

44 **Supplementary Figure 1. Characterization of CD20^{dim} CD4⁺T cell subpopulation.** **A.** Left,
45 gating strategy used to identify CD20^{dim} cells, with and without inclusion of the CD19 marker.
46 Previous sequential gates are represented in Supplementary Figure 9. Right, comparison of
47 percentages of the CD20^{dim} CD4⁺ T cell population with or without B cell exclusion in n=3 ART-
48 suppressed patients. **B.** Representative bright-field and color fluorescence images of T-B cells
49 conjugates found in the CD20^{high} CD4⁺ T cell population of ART-suppressed patients (#9 and 22).
50 Percentage of singlet (dark orange) and doublet (light orange) events among total nucleated
51 events detected in each population. Individual graphs from each ART-suppressed patients. Scale
52 bar 10 μ m. **C.** CD20-mRNA was measured in sorted CD20^{dim} CD4⁺T cells (orange) and CD20⁻ CD4⁺T
53 cells (black). Relative expression of CD20-mRNA to β -actin-mRNA of n=3 ART-suppressed
54 patients (#49-51), arbitrary units (AU). **D.** Characterization of follicular helper cells (T_{FH})
55 phenotype defined by CXCR5 and PD-1 expression in CD20⁻ or CD20^{dim} CD4⁺ T cells. Left, gating
56 strategy used to determine CXCR5 and PD-1 expression. Right, expression of CXCR5 and PD-1 in
57 CD20^{dim} and CD20⁻ CD4⁺ T cells in n=5 ART-suppressed (#17-19, 54 and 55, orange) and n=1
58 viremic (#86, red) patients. Wilcoxon comparison test was performed. Data underlying this
59 Figure is provided as Source Data file.

60

61

62

63

64

65

66

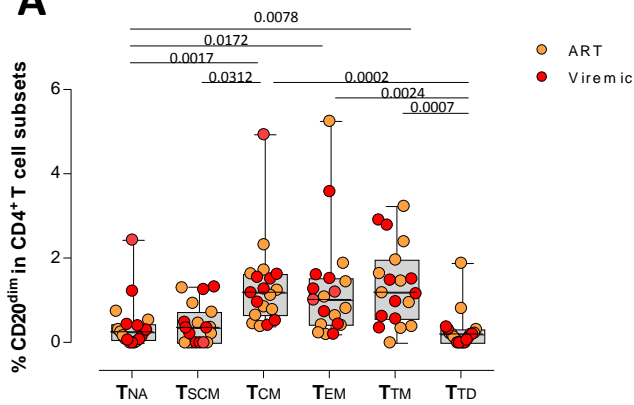
67

68

Supplementary Figure 2

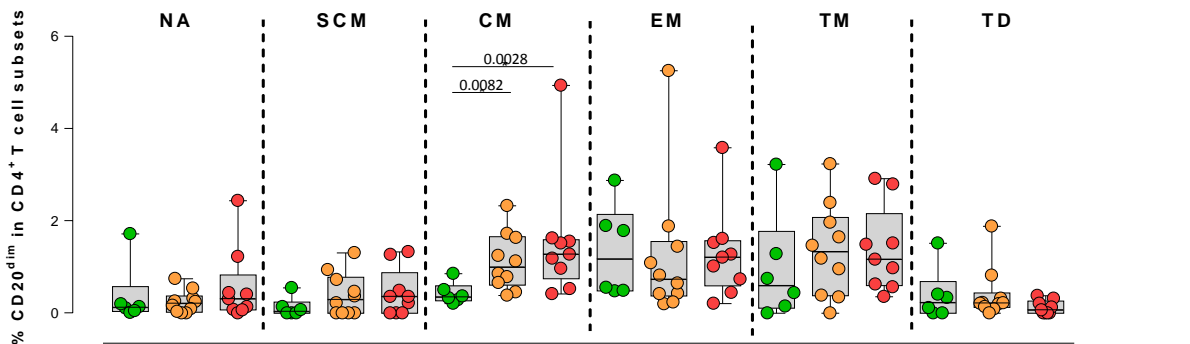
69

A

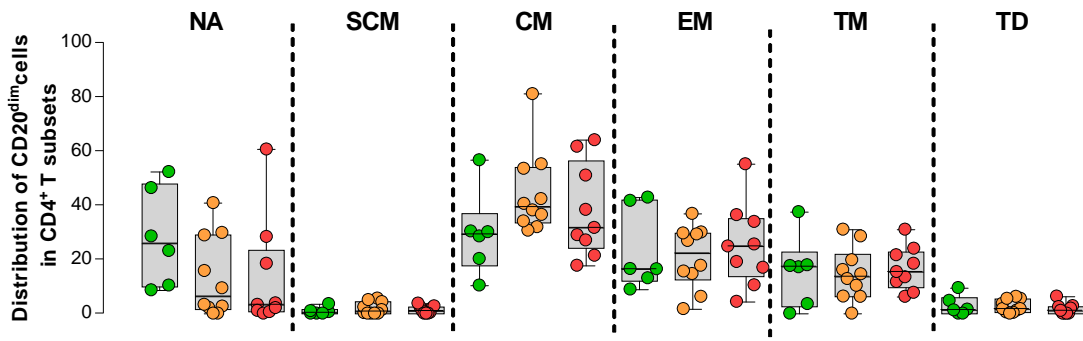


74

B

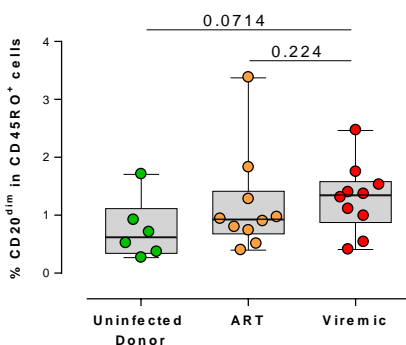


79



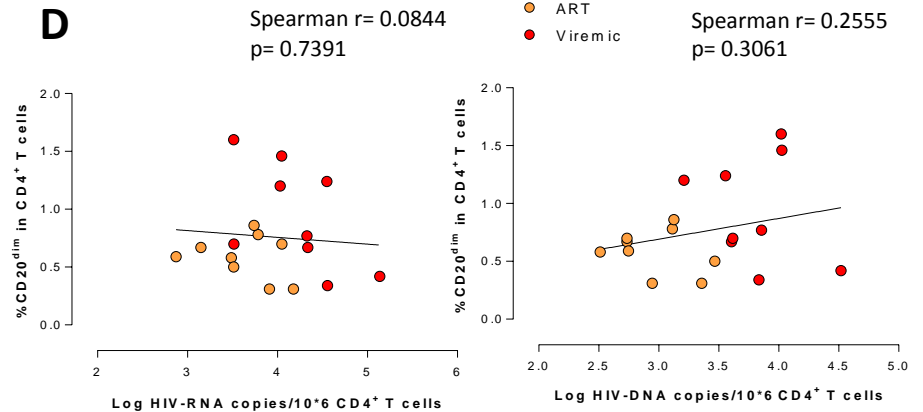
83

C



86

D



87

88 **Supplementary Figure 2. Expression and distribution of CD20^{dim} cells in CD4⁺ T cell subsets.**
89 **A.** Frequency of CD20^{dim} cells in T cell subsets of viremic (red) and ART-suppressed (orange)
90 individuals. ANOVA and Dunn's multiple comparison test were performed. **B.** The upper panel
91 shows percentages of expression of CD20^{dim} in CD4⁺ T cell subsets. The lower panel shows the
92 distribution of CD20^{dim}-expressing cells in different CD4⁺ T cell subsets. In both panels, the
93 median of uninfected donors, HIV⁺ ART-suppressed patients and HIV⁺ viremic patients is
94 presented. Mann-Whitney test. In panels A and B, patients #1-10, 60-65, 67-69 are represented,
95 n=6 HIV⁻ donors, n=10 ART-suppressed patients, n=9 viremic patients. **C.** Percentage of CD4⁺ T
96 memory subsets (defined as CD45RO⁺ cells) expressing CD20^{dim} in different cohorts of patients.
97 Panels A-C median and min-max rank are represented. **D.** Correlation of CD20^{dim} CD4⁺ T cells
98 with intracellular HIV RNA (left) and total HIV DNA (right) are shown. Data from n=9 ART-
99 suppressed (#2-10, orange) and n=9 viremic (#60-65, 67-69, red) patients are included.
100 Spearman's nonparametric correlation coefficients and associated *P* values are shown. Gating
101 strategy used for these analyses is shown in Figure 1A. Data underlying this Figure is provided
102 as Source Data file.

103

104

105

106

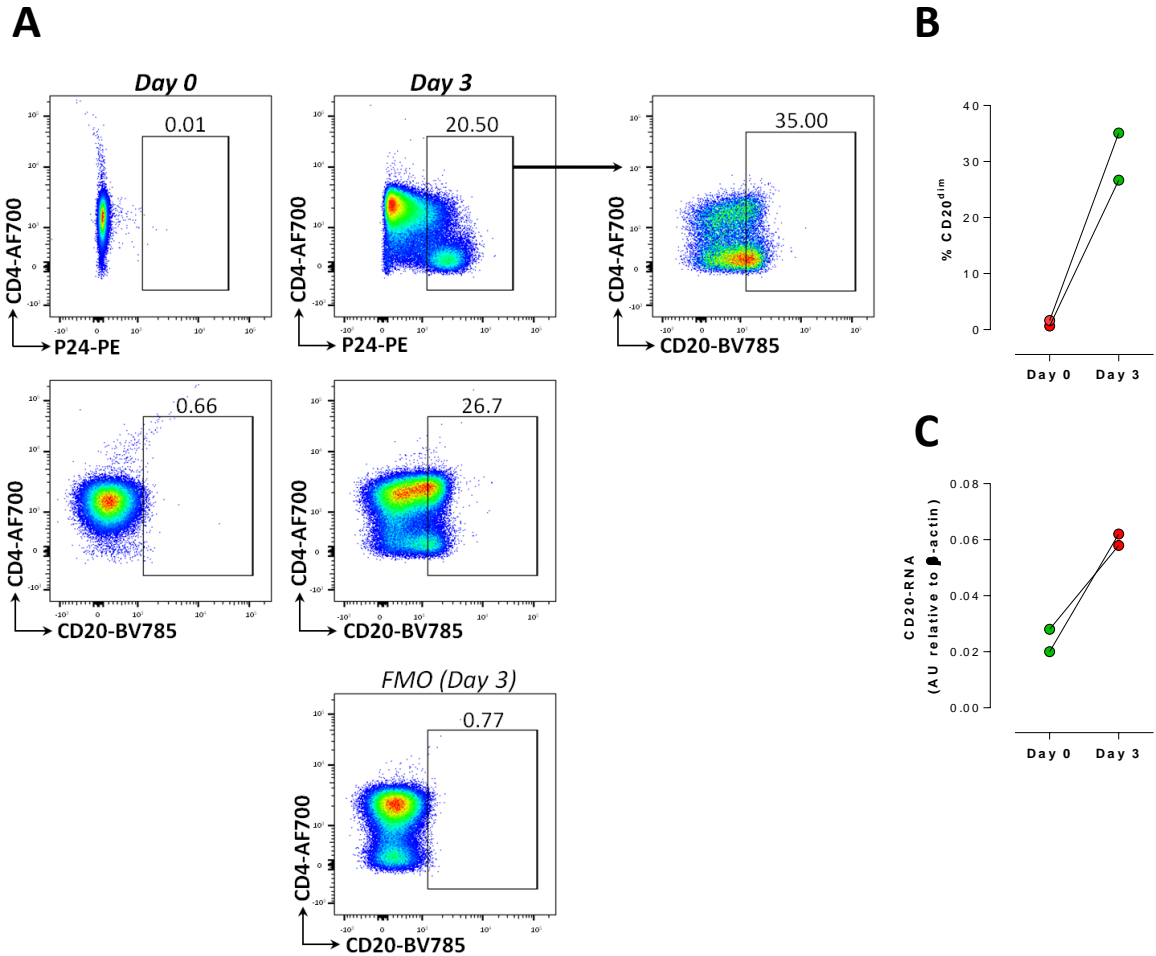
107

108

109

110

Supplementary Figure 3

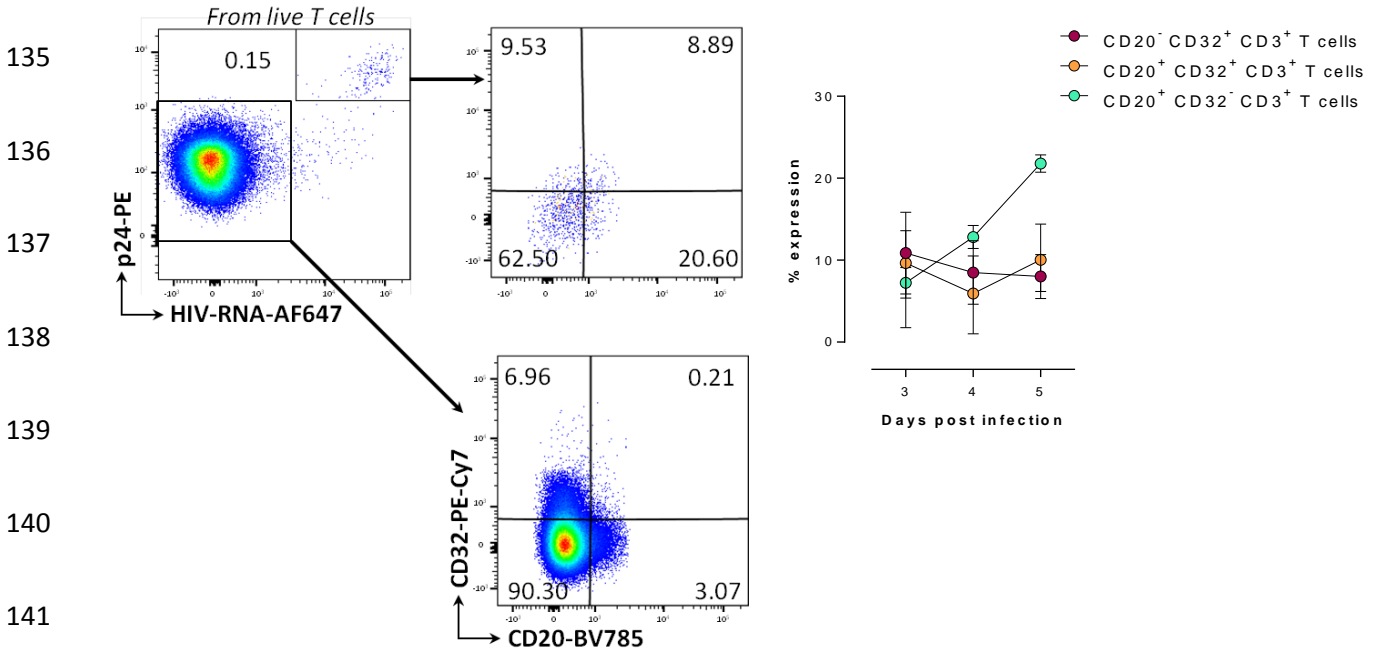


Supplementary Figure 3. Upregulation of CD20 expression after ex vivo HIV infection in previously isolated CD20⁻ CD4⁺ cells. CD4⁺ T cells non-expressing CD20 were isolated by cell sorting. The next day, cells were infected with the NL4.3 viral strain. CD20 expression was measured by flow cytometry and mRNA quantification at day 0 and 3 post-infection. **A.** Gating strategy used to identify p24⁺ cells (upper panel) and CD20 expression (lower panel). Previous sequential gates are represented in Supplementary Figure 9. **B.** Percentages of cells expressing CD20 in CD4⁺ T cells before and after infection. **C.** CD20-RNA levels after ex vivo infection. Relative expression of CD20-mRNA to β-actin-mRNA, arbitrary units (AU), from n=2 ex vivo infected cells. Data underlying this Figure is provided as Source Data file.

133

Supplementary Figure 4

134



138

Supplementary Figure 4. Expression of CD20 and CD32 in ex vivo-infected cells.

139 Unstimulated PBMCs from three uninfected donors were infected with the HIV strain NL4.3.

140 Infection was monitored by the simultaneous staining of HIV RNA using the RNA FISH-flow assay

141 and the viral protein p24 at days 3, 4 and 5 after infection. The left panel shows the gating

142 strategy used to monitor HIV infection and expression of CD20 and CD32. Previous sequential

143 gates are represented in Supplementary Figure 9. The right panel shows the percentage of

144 productively HIV-infected cells with CD20, CD32, and double-positive expression. Mean and SEM

145 are presented from 3 independent experiments. Data underlying this Figure is provided as

146 Source Data file.

147

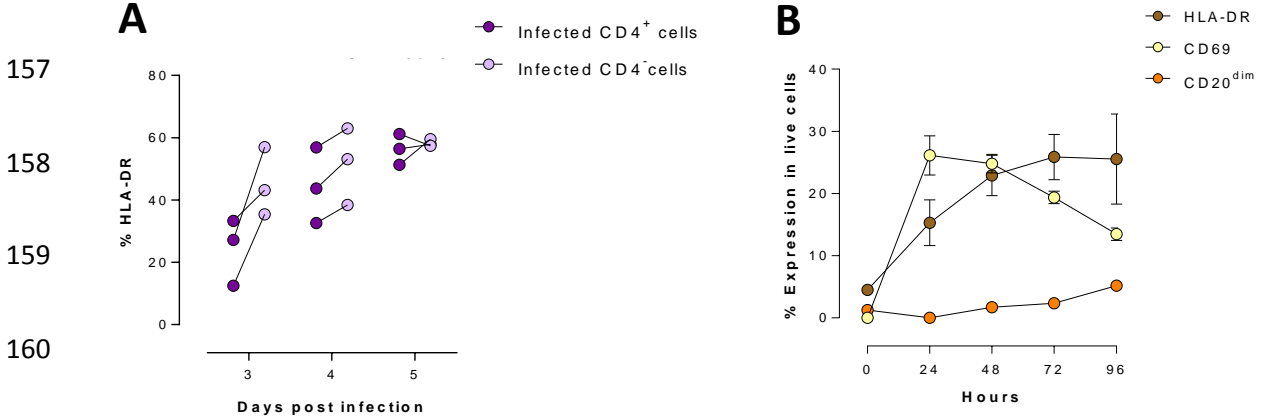
148

149

155

Supplementary Figure 5

156



160

161

162 **Supplementary Figure 5. Expression of HLA-DR in ex vivo-infected cells and expression of**

163 **CD20 during activation of CD4⁺ T cells. A.** Frequency of HLA-DR in HIV-infected cells at days 3, 4

164 and 5 after ex vivo infection of unstimulated PBMCs from three uninfected donors. **B.** Frequency

165 of CD20^{dim}, HLA-DR and CD69 in PBMCs from uninfected donors after stimulation with anti-CD3

166 (1 µg/ml) and anti-CD28 (2 µg/ml) for 96 h. Mean and SD are presented from 3 independent

167 experiments for HLA-DR and PD-1, and one experiment for CD20. Flow gating strategy is shown

168 in Figure 5. Data underlying this Figure is provided as Source Data file.

169

170

171

172

173

174

175

176

177

Supplementary Figure 6

178

179

180

181

182

183

184

185

186

187

188

189

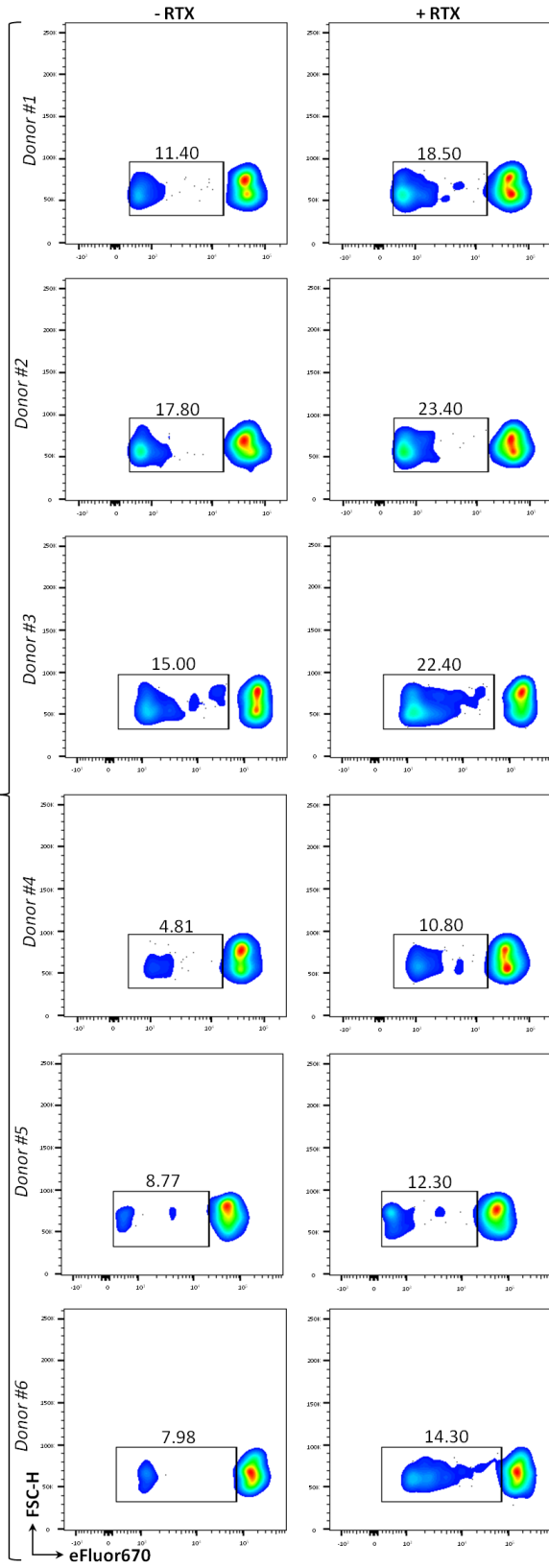
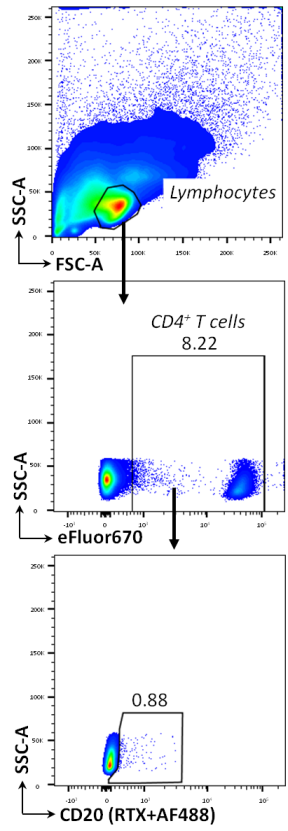
190

191

192

193

194



195

Supplementary Figure 6. Gating strategy for detection of ADCC in CD20^{dim} CD4⁺ T cells

196

induced by Rituximab. Flow gating strategy used to identify cell cytotoxicity in the samples from

197

6 individuals are shown.

198

Supplementary Figure 7

Patient #52

Patient #53

Patient #59

199

200

201

202

203

204

205

206

207

208

209

210

211

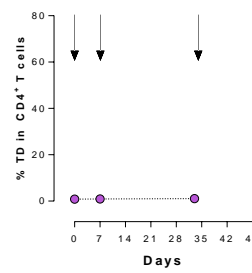
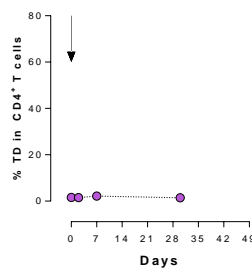
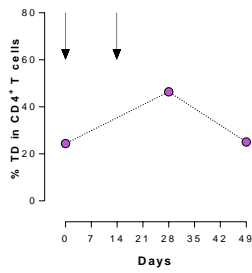
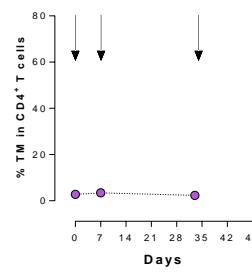
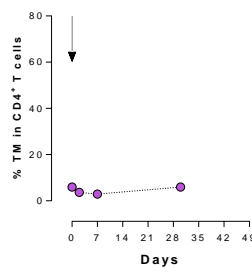
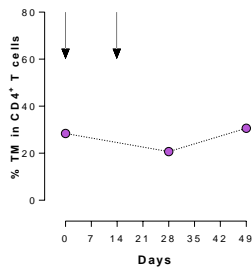
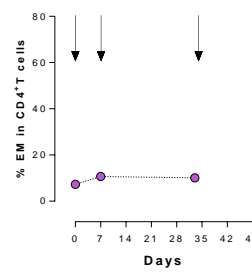
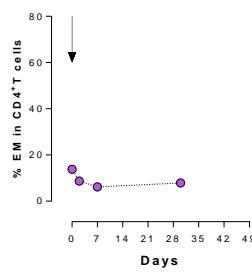
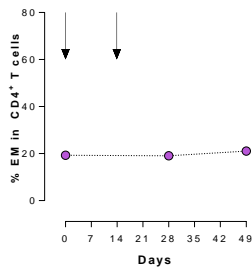
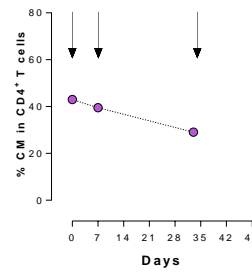
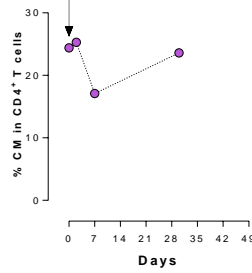
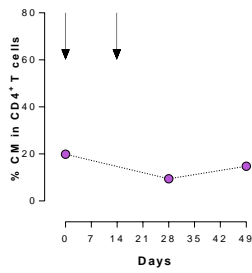
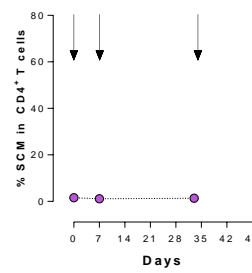
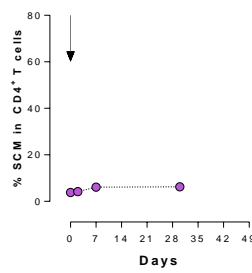
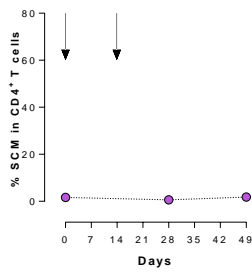
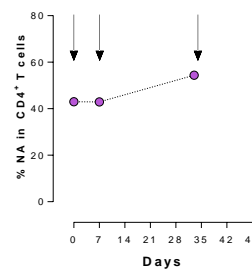
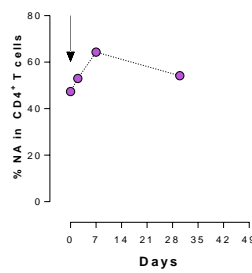
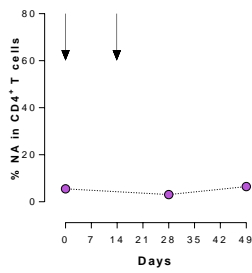
212

213

214

215

216



217 **Supplementary Figure 7. Longitudinal changes in the proportion of CD4⁺ T cell subsets after**
218 **in vivo administration of Rituximab.** Percentage of Naive (CCR7⁺, CD45RO⁻, CD27⁺, CD95⁻),
219 Memory Stem cells (CCR7⁺, CD45RO⁻, CD27⁺, CD95⁺); Central memory (CCR7⁺, CD45RO⁺)Effector
220 memory (CCR7⁻, CD45RO⁺, CD27⁻), Transitional memory (CCR7⁻, CD45RO⁺, CD27⁺); and
221 Terminally differentiated (CCR7⁻, CD45RO⁻) in CD4⁺ T cells are represented for patients, #52, #53
222 and #59. Flow gating strategy is shown in Figure 5. Data underlying this Figure is provided as
223 Source Data file.

224

225

226

227

228

229

230

231

232

233

234

235

236

237

238

239

Supplementary Figure 8

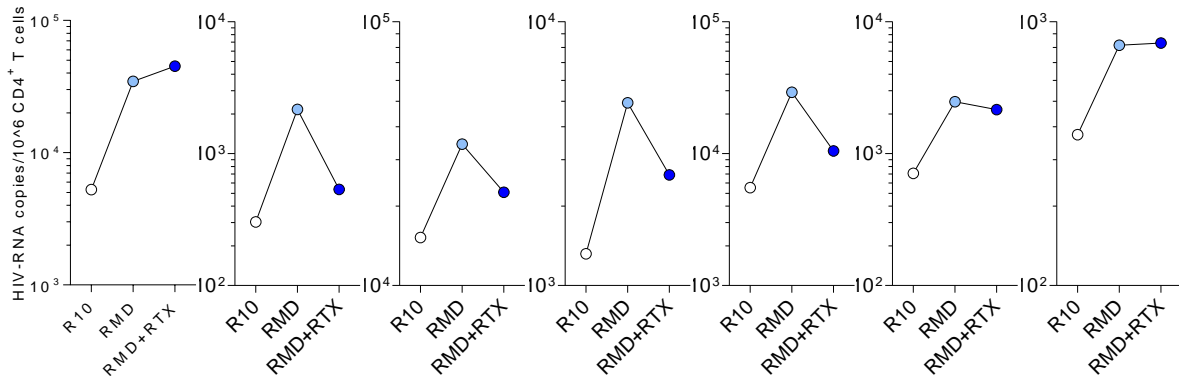
240

241

242

243

244



245

246

Supplementary Figure 8. Depletion of HIV RNA expressing cells by Rituximab after LRA

247

treatment. Unfractionated PBMCs from ART-suppressed patients were treated with latently

248

reversal agents (LRAs) romidepsin for 24h, and with Rituximab for 48h HIV RNA expression was

249

measured by qPCR. The individual data for the HIV RNA quantification before and after viral

250

reactivation with the addition of a control antibody or Rituximab in responder patients are

251

shown. Patients #23 and 42-47. Data underlying this Figure is provided as Source Data file.

252

253

254

255

256

257

258

259

260

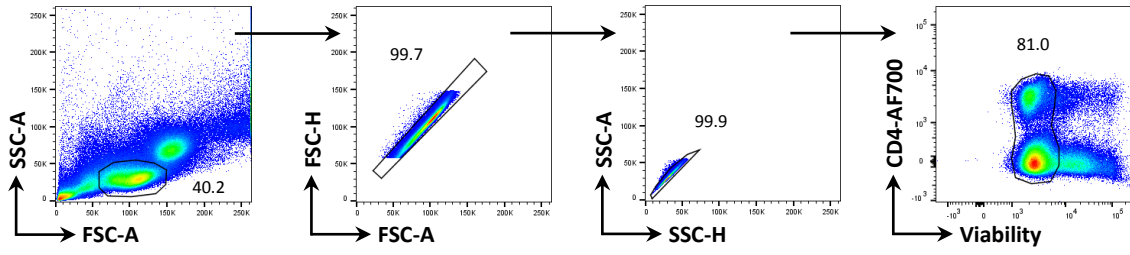
Supplementary Figure 9

261

262

263

264



265

Supplementary Figure 9. Sequential flow gating strategy used in Figures 1, 2, 5, 6 and 7, and

266

Supplemental Figures 1, 2, 3, 4, 5 and 7.